Cellular/Molecular

The Endogenous Redox Agent L-Cysteine Induces T-Type Ca^{2+} Channel-Dependent Sensitization of a Novel Subpopulation of Rat Peripheral Nociceptors

Michael T. Nelson,[1,3] Pavle M. Joksovic,[1] Edward Perez-Reyes,[2,3] and Slobodan M. Todorovic[1,3]

Departments of [1]Anesthesiology and [2]Pharmacology and [3]Neuroscience Graduate Program, University of Virginia School of Medicine, Charlottesville, Virginia 22908

Recent studies have demonstrated a previously unrecognized contribution of T-type Ca^{2+} channels in peripheral sensory neurons to pain sensation (nociception). However, the cellular mechanisms underlying the functions of these channels in nociception are not known. Here, in both acutely dissociated and intact rat dorsal root ganglion neurons, we characterize a novel subpopulation of capsaicin- and isolectin B_4-positive nociceptors that also expresses a high density of T-type Ca^{2+} currents. Using these "T-rich" cells as a model, we demonstrate that the endogenous reducing agent L-cysteine lowers the threshold for nociceptor excitability and induces burst firing by increasing the amplitude of T-type currents and shifting the gating parameters of T-type channels. These findings, which provide the first direct evidence of T-type Ca^{2+} channel involvement in the control of nociceptor excitability, suggest that endogenous T-type channel agonists may sensitize a unique subpopulation of peripheral nociceptors, consequently influencing pain processing under normal or pathological conditions.

Key words: **low-threshold calcium channel; calcium; dorsal root ganglion; pain; thalamus; serotonin**

Introduction

It is generally known that peripheral pain transmission can be influenced by naturally occurring substances having the ability to decrease the threshold for pain fiber activation. The electrophysiological correlates of these altered pain responses, or sensory plasticity, collectively termed sensitization, include lower thresholds for activation, increased frequency of firing in response to suprathreshold stimuli, and spontaneous firing (Levine et al., 1993; Caterina and Julius, 2001; Bhave and Gereau, 2004). When nociceptors are in a heightened state of sensitivity, they often respond to normally innocuous stimuli by producing pain (allodynia) and to normally painful stimuli in an exaggerated manner (hyperalgesia). Although it is known that sensitization of nociceptors contributes to various pain pathologies, the precise cellular mechanisms underlying sensitization are unclear. Previous studies have demonstrated that the endogenous reducing agent L-cysteine augments T-type currents in nociceptive neurons *in vitro* (Todorovic et al., 2001) and produces peripheral sensitization to thermal and mechanical stimuli *in vivo* (Todorovic et al., 2001, 2004a). Despite these interesting findings, the precise contributions of T-type channels to nociception remain elusive.

In vitro studies have described the presence of T-type currents in small dorsal root ganglion (DRG) cells (Schroeder et al., 1990; Scroggs and Fox, 1992; Todorovic and Lingle, 1998), most of which are nociceptors (Levine et al., 1993; Snider and McMahon, 1998; Caterina and Julius, 2001). More recent functional studies have also indicated that T-type channels contribute to nociception, suggesting that these channels may amplify pain signals from the periphery (Todorovic et al., 2001, 2004a,b; Bourinet et al., 2005). Because T-type Ca^{2+} channels act over a range of membrane potentials near the resting potential of many cells, it has been suggested that these channels may influence pain sensation by altering the excitability parameters of nociceptors. However, this intriguing hypothesis has not been demonstrated conclusively.

In the present study, we characterize a novel subpopulation of small capsaicin-sensitive and isolectin B_4 (IB_4)-positive DRG cells that expresses prominent T-type currents ("T-rich" cells). We show in these cells that L-cysteine lowers the threshold for excitability and induces T-type Ca^{2+} channel-dependent burst firing. Finally, we use a combination of electrophysiological and computer-modeling methods to demonstrate that the L-cysteine-evoked enhancement of excitability may be the result of gating shifts in the availability of T-type channels for activation. This study therefore provides the first direct demonstration of T-type Ca^{2+} channel involvement in the control of nociceptor excitability. Our results also suggest that endogenous T-type Ca^{2+} channel agonists may sensitize a distinctive subpopulation of peripheral nociceptors, consequently influencing pain processing under normal or pathological conditions.

Received June 20, 2005; revised Aug. 5, 2005; accepted Aug. 5, 2005.

This work was supported by grants from the National Institute on Drug Abuse (K08-DA00428) and the National Institute of General Medical Sciences (R01GM070726) to S.M.T. We thank Dr. Steven Mennerick, Elena van der Schalie, and Le Peng, for helpful comments on this manuscript and Allison P. Berg for technical assistance.

Correspondence should be addressed to Dr. Slobodan M. Todorovic, Department of Anesthesiology, University of Virginia School of Medicine, Mail Box 800710, Charlottesville, VA 22908. E-mail: st9d@virginia.edu.

DOI:10.1523/JNEUROSCI.2527-05.2005

 0270-6474/05/258766-10$15.00/0

Materials and Methods

Acutely dissociated DRG neurons. Dissociated DRG cells were prepared from adolescent albino Sprague Dawley rats (60–150 g) and used within 8 h for whole-cell recordings as described previously (Todorovic and Lingle, 1998). In brief, 10–12 DRGs from thoracic and lumbar regions were dissected and incubated at 36°C for 60 min in Tyrode's solution containing (in mM) 140 NaCl, 4 KCl, 2 $MgCl_2$, 2 $CaCl_2$, 10 glucose, and 10 HEPES, adjusted to pH 7.4 with NaOH, and supplemented with 2 mg/ml collagenase H (Roche, Indianapolis, IN) and 5 mg/ml dispase I (Roche). After incubation, ganglia were washed three times with Tyrode's solution at room temperature. Single neuronal somata were then obtained at room temperature by a series of triturations through three glass pipettes fire-polished to progressively decreasing diameters. Using this method, we were able to exclude most large (>45 μm) cells, most of which contribute little to nociception. For recordings, cells were plated onto an uncoated glass coverslip, placed in a culture dish, and perfused with external solution. All data were obtained from isolated cells without visible processes. All experiments were done at room temperature. We routinely observed small, T-rich, and medium cells in the same preparation (see Fig. 1). Varying the time of enzymatic treatment or the age of the animal (up to 6 months) did not significantly alter the percentage of each subtype observed or the effects of any drugs on T-type currents (data not shown).

Intact DRG preparation. DRGs were dissected with partial segments of both the peripheral nerve and spinal roots attached. Whole ganglia were then incubated at 36°C for 90 min in Tyrode's solution supplemented with 2 mg/ml collagenase H and 5 mg/ml dispase I. After incubation, ganglia were washed three times with Tyrode's solution at room temperature, and the overlying sheets of connective tissue were carefully removed. For recording, ganglia were transferred to a recording chamber and held in place with a platinum wire grid. The weight of the grid flattened ganglia, allowing visualization of individual cells along most of the periphery. Leaving segments of the peripheral nerves and spinal roots attached increased the contact area with the grid, resulting in greater stability for recording. Ganglia were visualized with an infrared differential interference contrast camera (C2400; Hammamatsu, Hammamatsu City, Japan) on a Zeiss (Jena, Germany) 2 FS Axioscope with a 40× lens. In this preparation, we again observed small, T-rich, and medium cells as well as many large cells previously excluded by the mechanical trituration process.

Electrophysiology. Recordings were made using standard whole-cell techniques. Electrodes were pulled from borosilicate glass microcapillary tubes (Drummond Scientific, Broomall, PA) and had resistances from 1 to 3 MΩ when filled with internal solution. We made recordings using an Axopatch 200B patch-clamp amplifier (Molecular Devices, Foster City, CA). Voltage and current commands and digitization of membrane voltages and currents were controlled using a Digidata 1322A interfaced with Clampex 8.2 of the pClamp software package (Molecular Devices), running on an IBM-compatible computer. We analyzed data using Clampfit (Molecular Devices) and Origin 7.0 (Microcal Software, Northampton, MA). Currents were low-pass filtered at 2–5 kHz. Series resistance (R_s) and capacitance (C_m) values were taken directly from readings of the amplifier after electronic subtraction of the capacitive transients. Series resistance was compensated to the maximum extent possible (usually 50–80%). In some experiments, we used a P/5 protocol for on-line leak subtractions. Action potentials were recorded in the fast current-clamp mode.

Multiple independently controlled glass syringes served as reservoirs for a gravity-driven local perfusion system. Manually controlled valves accomplished switching between solutions, except for applications of capsaicin and ATP, when we used electronically controlled valves (Valvelink 8; AutoMate Scientific, San Francisco, CA) for fast drug applications. Solution exchange was accomplished by constant suction through a glass capillary tube at the opposite end of the recording dish. All drugs were prepared as stock solutions: 1 mM TTX; 10 mM capsaicin, ATP, serotonin (5-HT), (3β,5α,17β)-17-hydroxyestrane-3-carbonitrile (ECN), and (3β,5β,17β)-3-hydroxyandrostane-17carbonitrile (3βOH); 100 mM L-cysteine, mibefradil, and Ni^{2+}; and 300 mM 5,5′-dithio-bis-(2-nitrobenzoic acid) (DTNB). The drugs were freshly diluted to the appropriate concentrations at the time of the experiments. TTX, ATP, 5-HT, L-cysteine, and Ni^{2+} were prepared in H_2O. L-Cysteine was used within 30 min of the final dilution because of instability resulting from spontaneous oxidation in the presence of trace-metal ions. Capsaicin, ECN, 3βOH, mibefradil, and DTNB were prepared in DMSO. The maximal concentration of DMSO in any one experiment was 0.5%. At this concentration, DMSO has no effect on Ca^{2+} currents or membrane potential (Todorovic et al., 2001). Mibefradil was a kind gift from Roche. ECN and 3βOH were generously provided by Dr. D. Covey (Washington University, St. Louis, MO).

For voltage-clamp experiments with dissociated cells, the external solution used to isolate Ca^{2+} currents contained the following (in mM): 10 $BaCl_2$, 152 tetraethylammonium (TEA)-Cl, and 10 HEPES, adjusted to pH 7.4 with TEA-OH. In recordings from intact ganglia, 2 mM Ca^{2+} was used in place of Ba^{2+}. The external solution used for all current-clamp and voltage-clamp recordings with capsaicin, ATP, and 5-HT contained the following (in mM): 140 NaCl, 4 KCl, 2 $MgCl_2$, 2 $CaCl_2$, 10 glucose, and 10 HEPES, adjusted to pH 7.4 with NaOH. The external solution used for Ca^{2+}-free recordings was the same minus Ca^{2+}. The internal solution used for all voltage-clamp recordings except isochronal recordings of activation tail currents contained the following (in mM): 110 Cs-methane sulfonate, 14 phosphocreatine, 10 HEPES, 9 EGTA, 5 Mg-ATP, and 0.3 Tris-GTP, adjusted to pH 7.3 with CsOH. To avoid any possible contamination of activation tail currents with even minimal high-voltage-activated (HVA) components, we used an F^--based internal solution to facilitate HVA rundown (in mM): 135 tetramethylammonium hydroxide, 10 EGTA, 40 HEPES, and 2 $MgCl_2$, adjusted to pH 7.2 with hydrofluoric acid. In these experiments, T-rich cells were identified by the current–voltage (*I–V*) signature rapidly after the transition to whole-cell configuration, before any substantial HVA rundown and possible mistaken classification could occur. The pipette solution used for all current-clamp recordings contained the following (in mM): 130 KCl, 5 $MgCl_2$, 1 EGTA, 40 HEPES, 2 Mg-ATP, and 0.1 Na-GTP, adjusted to pH 7.2 with KOH. All chemicals were obtained from Sigma (St. Louis, MO), unless noted otherwise.

Immunohistochemistry. After the positive identification of a T-rich cell by *I–V* signature, we exchanged the Ca^{2+} current-isolating external solution for Tyrode's solution supplemented with 10 μg/ml IB_4 (Sigma) (Stucky and Lewin, 1999) conjugated to green fluorescein isothiocyanate (FITC) (Sigma). The dish was then incubated in the dark for 10–12 min and subsequently rinsed three times with Tyrode's solution. Cells were visualized using a standard FITC filter. Only cells with an intense halo of stain around the plasma membrane were considered to be positive. Only one round of staining was done per dish. Classification of cells as positive or negative was made by an investigator blinded to the *I–V* signature of the cell.

Analysis. Unless indicated otherwise, statistical comparisons were made using Student's *t* tests. All data are expressed as means ± SEM. The percentage reductions in peak current at various Ni^{2+} concentrations were used to generate a concentration–response curve. Mean values were fit to the following Hill function:

$$PB([Ni^{2+}]) = PB_{max}/(1+([IC_{50}/[Ni^{2+}])^n), \quad (1)$$

where PB_{max} is the maximal percentage block of peak current, IC_{50} is the concentration that produces 50% inhibition, and n is the apparent Hill coefficient for blockade. The fitted value is reported with 95% linear confidence limits. The kinetics of current activation and inactivation were determined by fitting *I–V* waveforms with the following function (Hodgkin and Huxley, 1952):

$$I(t) = A\times(1-\exp(-t/\tau_m))^n\times\exp(-t/\tau_h), \quad (2)$$

where A is a scaling factor, τ_m is the time constant of activation, n is the number of particles involved in the activation process, and τ_h is the time constant of inactivation. The voltage dependencies of activation and steady-state inactivation were described with single Boltzmann distributions of the following forms:

$$\text{Activation: } I(V) = I_{max}/(1+\exp[-(V-V_{50})/k]) \quad (3)$$

$$\text{Inactivation: } I(V) = I_{max}/(1+\exp[(V-V_{50})/k]). \quad (4)$$

In these forms, I_{max} is the maximal activatable current, V_{50} is the voltage in which half of the current is activated or inactivated, and k is the voltage dependence (slope) of the distribution.

Computer modeling. The NEURON model uses mathematical descriptors of ionic conductances to calculate whether a channel is open as a function of voltage by applying Hodgkin–Huxley-type equations. Our simulations used the three-compartment, current-clamp version of this model as originally described for thalamocortical neurons (Destexhe et al., 1998). The maximum permeability of T-type channels was left as in the original model. The experimentally determined values of T-type currents in T-rich cells (see Fig. 7) were then used to replace the existing parameters for T-type channels in the model. The model was also corrected *post hoc* for a liquid junction potential (−7.7 mV) (see Fig. 7 for uncorrected data) and surface charge screening [−12.3 mV (Wilson et al., 1983)]. Experimental data were collected at ~24°C, and the simulations were at 36°C; the model accounts for this difference using previously determined Q_{10} values (Coulter et al., 1989).

Results

T-rich cells represent a novel subtype of sensory neurons

The majority of nociceptive DRG fibers originate as free nerve endings in the skin; their central processes terminate in the dorsal horn of the spinal cord. However, their small size precludes any direct electrophysiological assessment of peripherally and centrally located ion channels that may contribute to nociception. Thus, cell bodies in the DRG, which can be easily isolated for electrophysiological examination, are often used as *in vitro* models to study nociception and other forms of sensory processing.

Several studies have documented differences in voltage-gated Ca^{2+} current (VGCC) expression between distinct subpopulations of acutely dissociated DRG neurons. Nearly all DRG cells contain HVA currents (Scroggs and Fox, 1992), which are thought to have an important function in synaptic transmission (Miller, 1998; Catterall, 2000). However, expression of T-type Ca^{2+} current is more heterogeneous between large (>45 μm in diameter), medium (32–45 μm), and small (20–30 μm) DRG cells (Scroggs and Fox, 1992). Based on studies using intact DRG–peripheral nerve preparations, it is generally thought that most small and some medium DRG cells contribute to nociception (Lee et al., 1986). Thus, we restricted our experiments to cells <45 μm in diameter ($n = 295$).

To assess the variety of VGCCs present in each subtype, we collected *I–V* data by voltage clamping cells at −90 mV and applying a series of depolarizing steps from −80 to +50 mV in 5 mV increments. Small cells expressed moderate (up to 1.5 nA) T-type currents at hyperpolarized potentials and large HVA currents at more depolarized potentials (Fig. 1*A*). Medium cells expressed very large (up to 7 nA) T-type currents and equally prominent HVA currents (Fig. 1*C*). These results are very similar to those reported previously for small and medium cells (Schroeder et al., 1990; Scroggs and Fox, 1992). Interestingly, we also observed a subset of small cells (26–31 μm) with large T-type currents (up to 3 nA) but virtually no HVA currents throughout the entire range of examined potentials (Fig. 1*B*). We compared these unique small cells, which, for clarity, we designated as T-rich, with classically described small and medium cells.

To analyze *I–V* relationships across all examined potentials, peak currents were normalized, averaged, and plotted versus test potential. The *I–V* curves for small and medium cells peaked at −5 and −10 mV, respectively, illustrating the contribution of substantial HVA currents (Fig. 1*D*,*F*). Conversely, the *I–V* curve for T-rich cells showed a substantial leftward shift to more hyperpolarized potentials and a peak at −30 mV, reflecting the predominance of T-type currents in these cells (Fig. 1*E*).

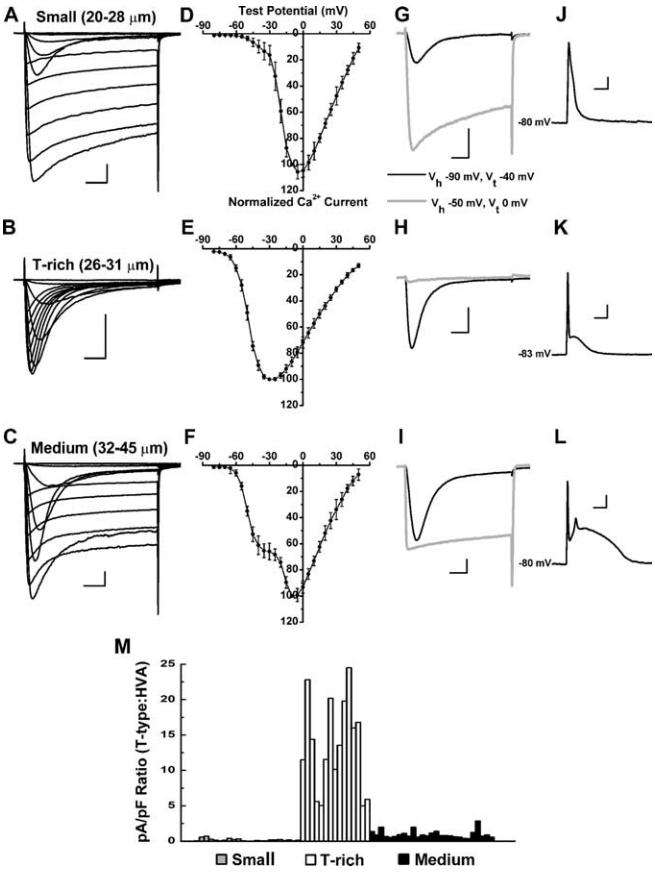

Figure 1. T-rich cells express a unique profile of voltage-gated Ca^{2+} currents. ***A–C***, Families of Ca^{2+} currents evoked in representative small ($R_s = 3.1$ MΩ, $C_m = 15.6$ pF), T-rich ($R_s = 1.8$ MΩ, $C_m = 30.2$ pF), and medium ($R_s = 2.3$ MΩ, $C_m = 38.5$ pF) cells, by voltage steps from −90 mV (V_h) to −80 (V_t) through +30 mV in 10 mV increments. Note that in small and medium cells, both T-type (rapidly inactivating) and HVA (slowly inactivating) currents are present but that in T-rich cells, the currents are almost exclusively of the T type. The *I–V* curve for medium cells also displays a characteristic shoulder (Scroggs and Fox, 1992) at hyperpolarized potentials because of the influence of very large T-type currents. Recordings were made in a single dish. For consistency in classification, a cell was only considered T-rich only if it possessed <300 pA of noninactivating current at the end of the V_t of 0 mV. ***D–F***, Normalized peak currents activated at the indicated test potentials. All points are the mean values from 24, 49, and 30 cells, respectively. ***G–I***, Representative traces showing the currents evoked from the indicated V_h and V_t in representative small (***G***; $R_s = 1.9$ MΩ, $C_m = 17.3$ pF), T-rich (***H***; $R_s = 3.4$ MΩ, $C_m = 27.2$ pF), and medium (***I***; $R_s = 3.3$ MΩ, $C_m = 39.0$ pF) cells. ***J–L***, Representative current-clamp traces showing APs elicited at the indicated membrane potentials. We held cells at relatively hyperpolarized potentials at which ADP is prominent (−75 to −90 mV) by constant-current injection and applied 1 ms, 3–5 nA depolarizing pulses to elicit APs. We used this brief pulse to avoid contaminating APs and ADPs with the stimulus waveform. ***M***, Histogram showing the density ratio of T-type to HVA currents for a total of 65 small, T-rich, and medium cells ($n = 23$, 15, and 27 cells, respectively). Peak T-type currents in small cells averaged 539 ± 61 pA (25 ± 2 pA/pF); peak HVA currents averaged 4269 ± 518 pA (209 ± 27 pA/pF) ($n = 23$). Medium cells averaged 3804 ± 263 pA (115 ± 7 pA/pF) of peak T-type current and 4492 ± 318 pA (137 ± 10 pA/pF) of peak HVA current ($n = 27$). In contrast, peak T-type currents in T-rich cells averaged 2525 ± 262 pA (93 ± 8 pA/pF), whereas peak HVA averaged just 237 ± 53 pA (9 ± 2 pA/pF) ($n = 15$). Horizontal calibration bars: ***A–C***, ***G–I***, 25 ms; ***J–L***, 10 ms. Vertical calibration bars: ***A–C***, ***G–I***, 750 pA; ***J–L***, 20 mV.

To more accurately determine the relative amounts of T-type and HVA current present in each subtype, we measured the peak current elicited from holding (V_h) and test potentials (V_t) that produced near-maximal activation of T-type or HVA currents and, at the same time, biased one current type over the other (Fig. 1*G–I*). We then calculated the individual current density ratios of T-type currents ($V_h = -90$, $V_t = -40$ mV) to HVA currents

($V_h = -50$, $V_t = 0$ mV) in these cells ($n = 65$) (Fig. 1*M*). Medium cells had an average T-type versus HVA current density ratio of 1.0 ± 0.1, reflecting a nearly equal contribution of T-type and HVA currents to total Ca^{2+} current. Small cells had a ratio of 0.20 ± 0.03, reflecting a larger contribution of HVA versus T-type currents. In contrast, T-rich cells had an average ratio of 13 ± 2, illustrating the vast prevalence of T-type over HVA currents in these cells. Thus, T-rich cells are easily distinguished from medium cells on the basis of size and from both medium and previously described small cells by the level of HVA Ca^{2+} current expression.

Next we performed whole-cell, current-clamp experiments to examine the shape of the action potential (AP) in T-rich cells and to determine whether these cells also exhibit afterdepolarizing potentials (ADPs). Such potentials have been demonstrated previously only in some subsets of medium DRG cells (White et al., 1989). Small cells displayed broad APs (3.40 ± 0.04 ms duration measured at half-peak amplitude; $n = 16$) and no visible ADPs (Fig. 1*J*). In contrast, both T-rich cells (AP width, 1.20 ± 0.04 ms; $n = 15$) and medium cells (AP width, 0.96 ± 0.06 ms; $n = 15$) displayed narrower APs and prominent ADPs (Fig. 1*K*,*L*). To ensure correct cell identification in these experiments, we always obtained *I–V* data in Ca^{2+} current-isolating external solution after AP recording in current-clamp mode.

Intact DRG neurons have long afferent processes that are removed during mechanical dissociation. Thus, we asked whether the population of non-HVA-containing (T-rich) DRG cells could be explained by the loss of these processes in which HVA channels might be located. To address this possibility, we examined VGCCs in whole-cell recordings from an intact DRG preparation in which currents reflect both somatic and peripherally located channels. Figure 2, *A* and *B*, demonstrate that T-rich cells exist in intact DRG neurons in the same size range as those we observed in our dissociated preparations. T-type currents were present at negative membrane potentials, whereas stronger depolarizations elicited few, if any, sustained HVA currents.

The *I–V* distribution for T-rich cells in our whole-ganglia experiments (Fig. 2*C*) closely resembled the curve we obtained for dissociated T-rich cells (Fig. 1*E*). We also found that L-cysteine, an endogenous reducing agent and T-type channel agonist in sensory neurons (Todorovic et al., 2001), increased peak T-type current in intact T-rich cells by 47 ± 4% ($n = 4$; $p < 0.01$) (Fig. 2*D*). Because we were primarily interested in T-rich cells, we focused our experiments on intact DRGs to cells 26–31 μm. However, it is important to note that we also recorded several intact cells in the small ($n = 7$) and medium ($n = 8$) size range that contained both T-type and prominent HVA Ca^{2+} currents, indicating that they were very likely the same subtypes of small and medium cells we and others have observed in acutely dissociated preparations (data not shown). Together, these data indicate that acutely dissociated DRG cells accurately reflect the population of VGCCs expressed in intact DRGs. Furthermore, mechanical dissociation did not seem to alter the effects of reducing agents on T-type currents. However, as expected, drug delivery and voltage clamp were both compromised in intact preparations. For these reasons, we continued our detailed characterization of T-rich cells using acutely dissociated cells.

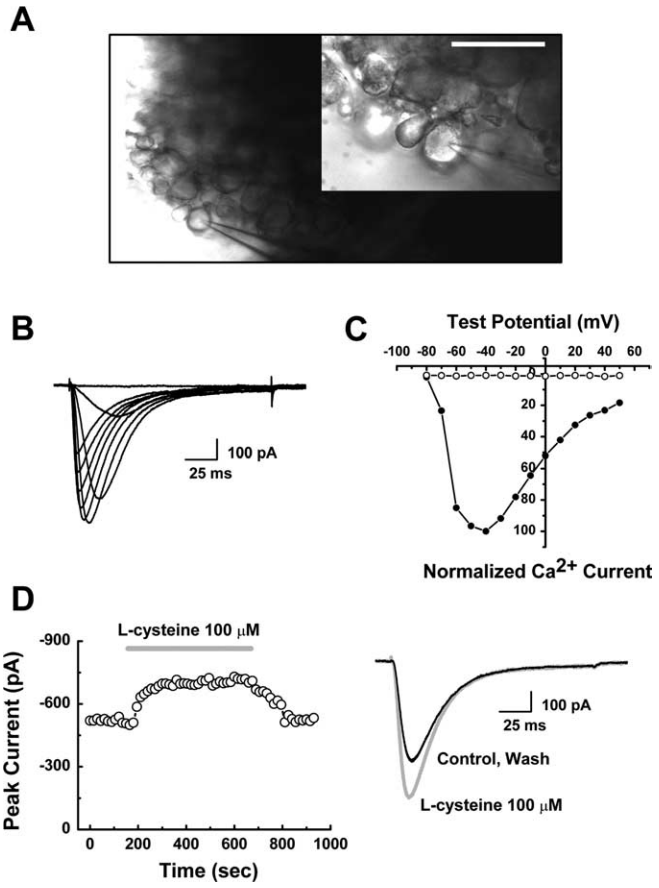

Figure 2. T-rich cells are present in intact DRGs. ***A***, Micrograph showing a representative T-rich cell on the periphery of an intact DRG preparation at low (100×) and high (400×) magnification. Scale bar: inset, 50 μm. ***B***, Representative family of currents evoked by voltage steps from a holding potential of −90 mV to test potentials from −80 to 0 mV in 10 mV increments ($R_s = 5.6$ MΩ, $C_m = 28.3$ pF). Data were obtained from the cell shown in ***A***. ***C***, Normalized currents activated at the indicated test potentials. Data show peak currents (filled circles) and noninactivating currents (open circles) measured at the end of the test pulse. All points are mean values from seven sets of *I–V* data obtained from a single T-rich cell. ***D***, Representative time course and raw traces showing the reversible increase in peak T-type current evoked by L-cysteine. Data were obtained from the cell shown in ***A***.

T-rich cells display nociceptive characteristics

Because T-rich cells are the same size as many nociceptors, we conducted experiments to determine whether these cells also express nociceptive characteristics. We first assayed for responsiveness to capsaicin, a principal marker of nociceptive function (Levine et al., 1993; Caterina and Julius, 2001). In voltage-clamp experiments, 89% ($n = 19$) of T-rich cells responded to 1 μM capsaicin, with an average inward current of 618 ± 132 pA (Fig. 3*A*, bottom trace). In current-clamp experiments, we also found that capsaicin depolarized T-rich cells (83%; $n = 18$) by 14 ± 6 mV (Fig. 3*A*, top trace). ATP has also been linked to pain, where it is believed to excite nociceptors after release from damaged tissues (McCleskey and Gold, 1999). All T-rich cells examined responded to 100 μM ATP with an average peak inward current of 805 ± 167 pA ($n = 6$) (Fig. 3*B*, bottom trace) and an average depolarization of 13 ± 2 mV ($n = 11$) (Fig. 3*B*, top trace).

The effect of 5-HT on DRG cells varies between different subpopulations. In larger, faster-conducting Aα- and Aβ-cells, 5-HT almost exclusively elicits depolarizing effects on membrane potential (Todorovic and Anderson, 1992; Cardenas et al., 1999). In contrast, experiments using intact DRG–sciatic nerve preparations have shown that in smaller, slower-conducting Aδ- and C-cells, 5-HT preferentially elicits hyperpolarizing effects on membrane potential (Todorovic and Anderson, 1992). Consistent with these findings, we observed hyperpolarizing responses to 10 μM 5-HT in the majority (60%) of T-rich cells ($n = 20$),

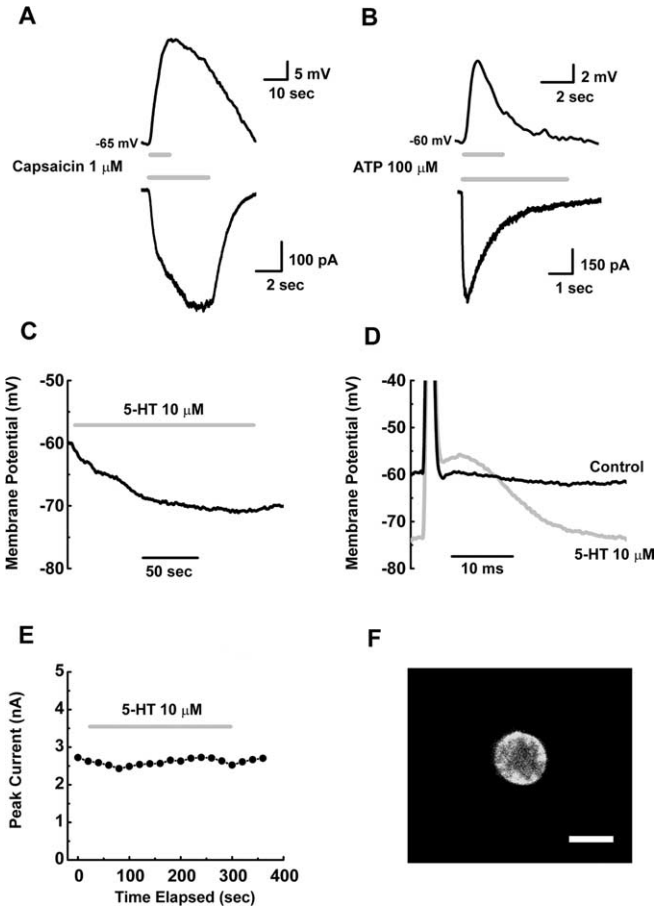

Figure 3. T-rich cells express nociceptive markers. ***A***, ***B***, Representative traces showing the response of T-rich cells to capsaicin (***A***; $R_s = 1.2$ MΩ, $C_m = 18.3$ pF) or ATP (***B***; $R_s = 1.8$ MΩ, $C_m = 28.3$ pF) recorded in both voltage-clamp (bottom traces) and current-clamp (top traces) mode. Because of contamination caused by intrinsic membrane fluctuations and switching between solutions, we considered cells to be responsive to capsaicin or ATP only if they evoked >50 pA of inward current under voltage clamp or 5 mV of depolarization under current clamp and the effect was reversed after removal of the agent. ***C***, Representative trace showing the hyperpolarizing effect of 5-HT on the natural membrane potential of a current-clamped T-rich cell ($R_s = 1.2$ MΩ, $C_m = 22.3$ pF). ***D***, Current-clamp traces from a representative T-rich cell showing the unmasking of the ADPP after membrane hyperpolarization by 5-HT. Spikes were elicited with 1 ms, 3 nA stimuli from the natural resting membrane potential. ***E***, Time course showing that 5-HT had no direct effect on the peak T-type currents in a representative T-rich cell ($R_s = 3.8$ MΩ, $C_m = 30.1$ pF). ***F***, Representative microphotograph of an IB_4-positive T-rich cell. Scale bar, 25 μm.

with an average hyperpolarization of 9 ± 1 mV (Fig. 3*C*). In current-clamp experiments using our AP stimulus, 5-HT was often able to hyperpolarize the membrane to levels that produced a deinactivation of T-type channels, as evidenced by unmasking of the ADP after the application of 5-HT (Fig. 3*D*). We examined the effects of 5-HT in voltage clamp and found no change in T-type current, suggesting that the effects of 5-HT on ADP are independent of any direct effect on T-type channels ($n = 4$) (Fig. 3*E*).

Nociceptors can also be classified by whether or not they bind the IB_4 from *Griffonia simplicifoilia*. Binding of IB_4 has been observed in subsets of both Aδ- and C-type nociceptors, as well as capsaicin- and ATP-positive cells (Stucky and Lewin, 1999; Petruska et al., 2000, 2002). Accordingly, we stained T-rich cells with IB_4 after identification on the basis of *I–V* signature and found that the majority (76%) of T-rich cells ($n = 17$) were IB_4 positve (Fig. 3*F*).

Because T-rich cells express such distinct voltage- and current-clamp profiles, we conducted experiments to assess whether the T-type currents in these cells respond to antagonists and agonists in the same manner as described previously for T-type currents in other nociceptive cells. T-type currents in T-rich cells were completely and reversibly blocked by Ni^{2+}, with a half-maximal block concentration (IC_{50}) of 29 ± 4 μM ($n = 10$; Hill coefficient, 1.09 ± 0.1; 95% block with 300 μM; data not shown). Conversely, L-cysteine reversibly increased peak T-type currents approximately twofold (81 ± 9%; $p < 0.001$; $n = 29$) in all T-rich cells tested, with a threshold around 10 μM and maximal effects near 100 μM (data not shown).

T-type Ca^{2+} currents modulate the excitability of T-rich cells

Although T-type channels have been implicated as influencing the excitability of many CNS neurons and some medium (White et al., 1989), presumably mechanoreceptive (Dubreuil et al., 2004), DRG cells, the role of these channels in the excitability of smaller capsaicin- and IB_4-positive cells has not been defined. This is of interest because changes in nociceptor excitability are thought to contribute to changes in pain sensation (Caterina and Julius, 2001). To address this question, we conducted current-clamp experiments on T-rich cells, which besides being small and capsaicin and IB_4 positive express virtually no HVA channels, and thus provide an added dimension of experimental control. L-Cysteine reversibly increased both the height (44 ± 4%) and width (53 ± 7%) of the ADP in all T-rich cells tested ($n = 31$; $p < 0.001$), with no visible effects on the initial AP spike (Fig. 4*A*). In addition, several T-rich cells fired in bursts after application of L-cysteine, demonstrating that in some cases, the augmented ADP resulted in a directly visible increase in somatic excitability (Figs. 4*A*, 5*A*,*B*,*E*). Switching to a Ca^{2+}-free external solution abolished the ADP, even in the continued presence of L-cysteine ($n = 4$) (Fig. 4*B*). In the presence of 500 nM tetrodotoxin (TTX) (used to partially isolate the ADP from the AP), L-cysteine increased both the height (46 ± 17%) and width (69 ± 19%) of the ADP ($n = 4$; $p < .01$) (Fig. 4*C*). Importantly, the effects of L-cysteine were independent of any shift in membrane potential or input resistance ($R_I = 343 \pm 75$ MΩ for control and 345 ± 69 MΩ with L-cysteine; $p > 0.05$; $n = 7$).

In our experiments, T-rich cells had an average resting membrane potential of −64 ± 5 mV ($n = 85$). Thus, we wanted to examine the ADP and the effects of L-cysteine at more physiological membrane potentials. As expected for a T-type channel-dependent phenomenon, the ADP was visible between membrane potentials of approximately −60 and −100 mV, with the size decreasing at the more depolarized potentials. L-Cysteine increased the ADP at all examined potentials and at −55 mV often produced a small depolarizing potential where there was none in control (Fig. 4*D*).

To assess the effects of L-cysteine on APs more directly, we conducted experiments on other small DRG cells with minimal T-type currents and thus no ADP. Figure 4*E* shows that in these cells, L-cysteine had no effect on AP shape, membrane potential, or R_I, even at fivefold increased concentrations ($n = 6$). This suggests that L-cysteine has little or no effect on the voltage-gated Na^+ and K^+ channels underlying the AP spike.

We next examined whether T-type channel antagonists and modulators could reverse the effects of L-cysteine: 100 μM Ni^{2+} (White et al., 1989; Todorovic and Lingle, 1998), 1 mM DTNB (Todorovic et al., 2001), 10 μM ECN (Todorovic et al., 1998), 1 μM 3βOH (Todorovic et al., 2004b), and 1 μM mibefradil (Todorovic and Lingle, 1998) are relatively selective for T-type Ca^{2+} channels over other voltage-gated ion channels in DRG

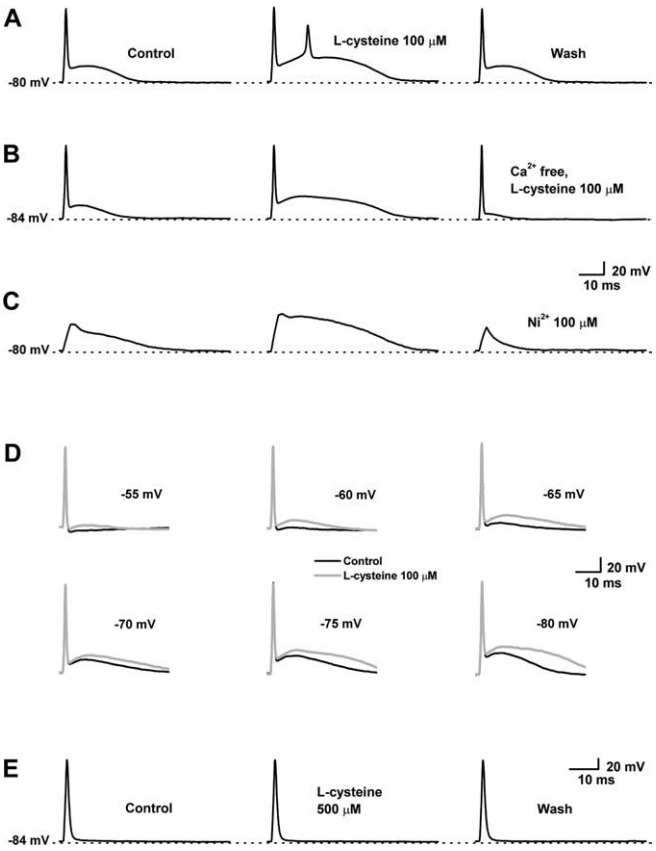

Figure 4. L-Cysteine increases excitability in T-rich cells. ***A***, Current-clamp traces from a T-rich cell showing the effects of L-cysteine on AP firing. Note that L-cysteine increases both the height and width of the ADP and induces a second AP spike. ***B***, The ADP is abolished in Ca^{2+}-free recording solution despite the continued presence of L-cysteine. ***C***, The effects of L-cysteine and Ni^{2+} on the ADP, which has been partially isolated by the addition of 500 nM TTX. ***D***, L-Cysteine increases the ADP in T-rich cells over a range of physiological membrane potentials. The third trace in the series (−65 mV) was recorded at the natural resting membrane potential of the cells. The traces at −55 and −60 mV and −70 to −80 mV were obtained by depolarizing or hyperpolarizing the membrane potential via commands delivered through the recording electrode. ***E***, L-Cysteine has no affect on APs in cells that do not contain T-type currents (no ADP), even at fivefold increased concentrations. The dotted lines represent the indicated voltages throughout the experiment.

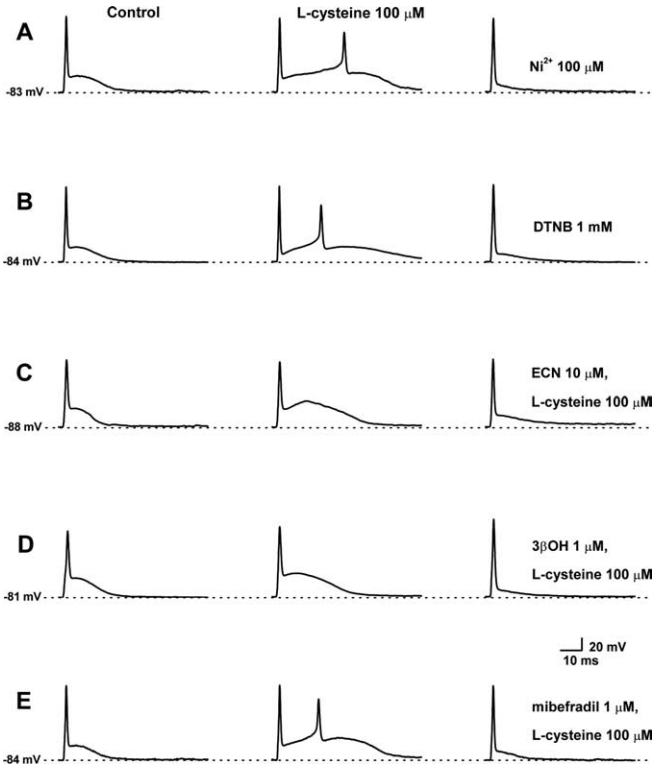

Figure 5. T-type antagonists reverse the effects of L-cysteine. ***A–E***, Current-clamp traces from five T-rich cells showing the effects of L-cysteine and various T-type antagonists on the ADP. The dotted lines represent the indicated voltages throughout the experiments. Note the occasional firing of a second AP in the presence of L-cysteine, with no shift in membrane potential. T-type antagonists reversed the effects of L-cysteine and blocked the ADP below control levels to the following degrees: Ni^{2+}, 65 ± 8% (height), 23 ± 4% (width), $n = 6$, $p < 0.01$; DTNB, 53 ± 7%, 36 ± 5%, $n = 4$, $p < 0.01$; ECN, 39 ± 8%, 24 ± 8%, $n = 4$, $p < 0.05$; 3βOH 46 ± 13%, 31 ± 10%, $n = 4$, $p < 0.05$; mibefradil, 71 ± 4%, 32 ± 3%, $n = 7$, $p < 0.01$. Ni^{2+} and DTNB were applied separately to avoid direct chemical redox interactions with L-cysteine.

neurons. In addition, our previous studies have shown that DTNB, ECN, 3βOH, and mibefradil induce analgesia when injected into the peripheral receptive fields of sensory neurons *in vivo*. Figure 5 shows that application of each of the aforementioned antagonists rapidly reversed the effects of L-cysteine and subsequently blocked the ADP below control levels. Additionally, all antagonists produced a reduction in ADP size when applied in isolation from L-cysteine to the following degrees: Ni^{2+}, 59 ± 9% (height), 29 ± 7% (width), $n = 4$, $p < 0.01$; DTNB, 48 ± 8%, 36 ± 6%, $n = 3$, $p < 0.05$; ECN, 46 ± 9%, 30 ± 6%, $n = 3$, $p < 0.05$; 3βOH, 38 ± 9%, 35 ± 15%, $n = 3$, $p < 0.05$; mibefradil, 66 ± 5%, 26 ± 2%, $n = 4$, $p < 0.01$ (data not shown).

Next we assessed whether L-cysteine lowers the threshold for excitability in T-rich cells. Figure 6*A* shows the results of a current-clamp experiment in which a reduced stimulus produced only a subthreshold depolarization under control conditions but a full AP and ADP in the presence of 100 μM L-cysteine. Ni^{2+} (100 μM) reversed the L-cysteine-evoked AP and blocked the initial depolarization, leaving only the stimulus transient remaining. Figure 6*B* shows consecutive segments from a similar experiment in which L-cysteine reversibly increased AP firing from subthreshold levels without shifting membrane potential. In similar experiments on nine T-rich cells, the probability of firing an AP increased to 75 ± 5% with L-cysteine from 10 ± 4% in control ($p < .001$). We excluded any cell with a membrane potential that spontaneously fluctuated >5 mV over the entire course of an experiment.

L-Cysteine modulates the gating parameters of T-rich cells

In an effort to identify the mechanism underlying the L-cysteine-evoked changes in excitability, we conducted voltage-clamp experiments to determine the effects of L-cysteine on various biophysical properties of T-type currents in T-rich cells. We determined the kinetics of current activation and inactivation from fits of a Hodgkin–Huxley model (Eq. 2) to currents elicited during 175 ms depolarizing steps to potentials between −50 and −10 mV (holding potential, −90 mV). L-Cysteine had no significant effect on activation time constants (τ_h) (Fig. 7*A*) but significantly accelerated inactivation time constants (τ_m) over the entire range of examined potentials (Fig. 7*B*). For example, at −50 mV, τ_m was 77 ± 14 ms in controls and 40 ± 7 ms in the presence of L-cysteine ($n = 7$; $p < 0.01$). Furthermore, L-cysteine had very little effect on T-type channel deactivation (Fig. 7*C*) or reactivation (recovery from inactivation) (Fig. 7*D*).

We then examined the effects of L-cysteine on voltage-dependent activation and inactivation in T-rich cells. L-Cysteine

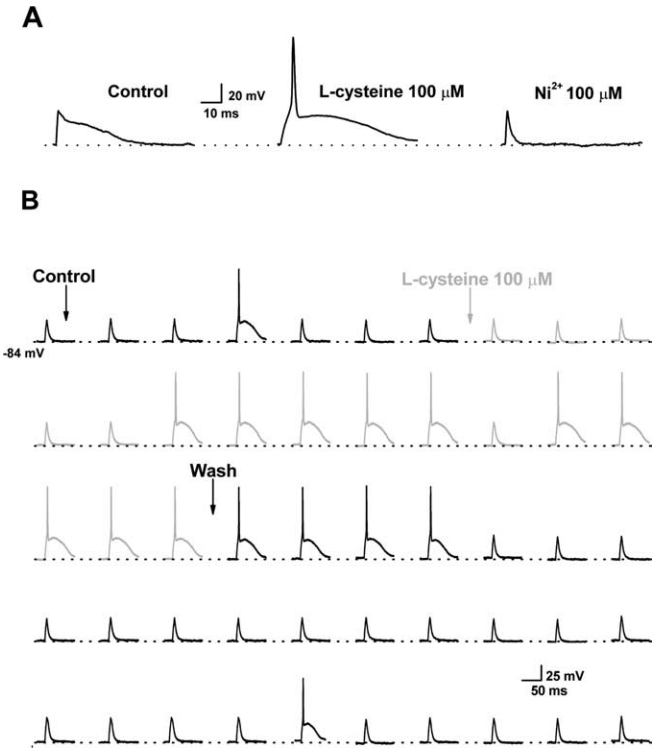

Figure 6. L-Cysteine lowers the threshold of excitability in T-rich cells. ***A***, Traces from a T-rich cell showing that a reduced stimulus (1 ms, 1.8 nA) elicited only subthreshold depolarization under control conditions but an AP and ADP after the addition of L-cysteine. Ni^{2+} reversed the effects of L-cysteine and blocked the subthreshold depolarization, leaving only the stimulus transient. ***B***, Continuous segment of a current-clamp experiment showing that the addition of L-cysteine rapidly and reversibly increased AP firing in a T-rich cell from subthreshold levels. The stimulus was 1 ms, 2 nA delivered every 10 s.

increased the peak of T-type current over the entire range of examined potentials but had a more prominent effect at negative potentials, causing a hyperpolarizing shift of ~5 mV ($n = 5$; $p < 0.001$) in the voltage dependence of activation (Fig. 7*E*). In contrast, there was a small depolarizing shift of ~2 mV in steady-state inactivation (Fig. 7*F*). Accordingly, L-cysteine evokes an increase in the "window period" (Fig. 7*G*) during which T-type channels are available for activation but have not yet been inactivated. The window period is operationally defined as the region of overlap beneath the Boltzmann distributions describing voltage-dependent activation and steady-state inactivation.

Thus, in addition to increased peak current, L-cysteine induces changes in the biophysical properties of T-type currents. It is possible that these changes alone could alter the excitability of T-rich cells. To examine the functional impact of the L-cysteine-induced gating shifts on excitability more closely, we modified a well established version of the NEURON model (Destexhe et al., 1998) to incorporate the biophysical parameters of T-type currents from T-rich cells. We then ran current-clamp simulations of subthreshold excitability, using a protocol similar to those in our *in vitro* current-clamp experiments. Under control conditions, the model predicted only a subthreshold potential. However, when the model was adjusted to reflect the sum gating effects of L-cysteine, the same stimulus was predicted to result in the firing of an AP (Fig. 7*H*). This prediction is nearly identical to the results we observed in our current-clamp experiments in both the absence and presence of L-cysteine. We then adjusted the model to reflect only the L-cysteine-evoked increase in window period, with all other parameters unchanged. Under these conditions, the model again predicted the firing of an AP with L-cysteine. These data indicate that T-type channels influence T-rich cell excitability and suggest that the effects of L-cysteine on voltage-dependent activation alone may be sufficient to lower the threshold for excitability in these cells.

Similar to our current-clamp experiments, our model simulations did not predict any L-cysteine-evoked membrane depolarization. This is somewhat intriguing, because an increase in window period would also be predicted to lead to an increase in steady-state window current and, potentially, membrane depolarization. However, T-type window currents are thought to be very small in amplitude (Perez-Reyes, 2003) and would likely result in only minor changes in membrane potential below the level of intrinsic fluctuations (usually between 0.5 and 2 mV, but up to 5 mV) that occur during even the most stable current-clamp recordings. Additionally, window currents are steady-state currents that build over time, but in our experiments, the effects of L-cysteine are rapid. We did not test the possibility that prolonged exposure to L-cysteine might induce small membrane depolarizations. Similarly, modeling does not take into account the duration of agonist application.

Discussion

Here, we have demonstrated that T-rich cells represent a novel subpopulation of T-type channel-containing peripheral nociceptors. T-rich cells express abundant T-type currents but virtually no HVA currents. To the best of our knowledge, this property is unique and distinguishes these cells from any previously described subpopulation of DRG neurons. This property also suggests that T-type channels are, overwhelmingly, the dominant routes of Ca^{2+} entry into these cells.

T-rich cells express a unique AP waveform within small DRG cells, the most prominent feature of which is a T-type channel-dependent ADP that is visible between membrane potentials of approximately −60 and −100 mV. The ADPs in T-rich cells were abolished in Ca^{2+}-free recording solution and inhibited by relatively selective antagonists of T-type channels, demonstrating that the ADP is both Ca^{2+}- and T-type channel dependent. The T-type currents in T-rich cells are sensitive to low concentrations of Ni^{2+}, with an IC_{50} value that is similar to the values reported for other nociceptive DRG cells (Todorovic and Lingle, 1998). In addition, T-rich cells, like most other small T-type channel-containing DRG cells, are responsive to capsaicin (Cardenas et al., 1995; Todorovic et al., 2001) and show a hyperpolarizing response to 5-HT. In contrast, medium DRG cells with prominent T-type currents and ADPs are unresponsive to capsaicin (Cardenas et al., 1995), show depolarizing responses to 5-HT (Cardenas et al., 1999), and express a high density of HVA currents (Scroggs and Fox, 1992; Cardenas et al., 1995; Dubreuil et al., 2004). These findings also support our assertion that T-rich cells are a distinct and unique subpopulation of DRG neurons.

T-rich cells express several principle characteristics of nociceptors, including responsiveness to capsaicin and ATP. The capsaicin-evoked currents we observed in T-rich cells displayed rapid onset and Ca^{2+}-dependent desensitization, properties that are characteristic of capsaicin-evoked currents in other DRG cells (Todorovic et al., 2001; Petruska et al., 2000, 2002), as well as recombinant cells expressing the capsaicin receptor (Caterina et al., 1997). The ATP-evoked currents were not only of similar magnitude to those that have been reported in several other nociceptor subpopulations (Petruska et al., 2000, 2002) but also had similar desensitization kinetics. Furthermore, T-rich cells are

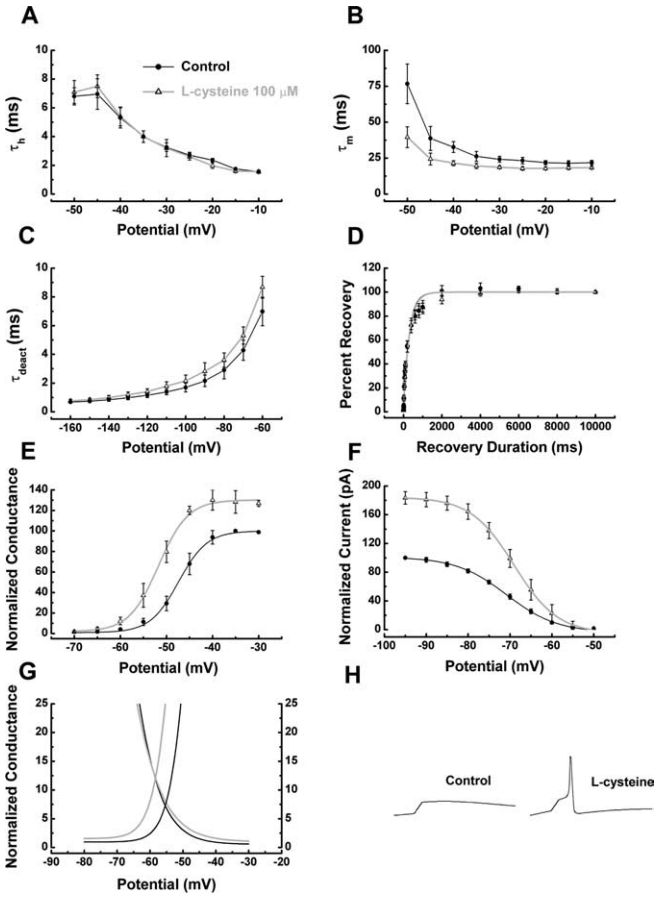

Figure 7. The effects of L-cysteine on the biophysical parameters of T-rich cells. ***A***, Mean activation time constants (τ_h) in the absence and presence of L-cysteine determined from fits of Equation 2 to currents activated by test pulses from −50 to −10 mV from a V_h of −90 mV ($n = 7$). Values for n ranged from 1.7 to 3.5. L-Cysteine had little effect on the kinetics of activation. ***B***, Mean inactivation time constants (τ_m) determined from fits of Equation 2 to the same currents shown in ***A***. L-Cysteine increased the rate of macroscopic inactivation over the entire range of examined potentials. ***C***, Mean time constants of deactivation determined from single exponential fits of tail currents plotted as a function of membrane potential ($n = 10$). The effects of L-cysteine on deactivation were examined at the indicated potentials after 20 ms depolarizing steps to −30 mV. Deactivation tail currents were reasonably well described by single exponential functions over this range. L-Cysteine has little effect on the kinetics of deactivation. ***D***, Mean reactivation (recovery from inactivation) plotted as a function of repolarization time at −90 mV ($n = 7$). Normalized data are fit with single exponential functions. Reactivation was examined with a paired-pulse protocol in which a 300 ms step to −30 mV was first used to inactivate most T-type current. After a variable recovery interval (2–10,000 ms) at −90 mV, a second step to −30 mV was used to assay the amount of current that had recovered. The percentage of recovery in the absence and presence of L-cysteine was then plotted as a function of recovery duration and fit with a single exponential function. ***E***, L-Cysteine shifts the voltage dependence of T-type channel activation to more hyperpolarized potentials. Data are mean values fit with Equation 3 ($n = 5$). Half-maximal activation (V_{50}) in control occurred at −47.4 ± 0.2 mV with a slope factor (k) of 3.1 mV. In the presence of L-cysteine, the V_{50} was −51.8 ± 0.2 mV with a k value of 3.2 mV. The voltage dependence of activation was determined using an isochronal tail– current protocol in which currents were measured at the end of a 20 ms depolarizing pulse to potentials between −70 and −30 mV ($V_h = -90$ mV). ***F***, L-Cysteine had little effect on the voltage dependence of inactivation. Data are mean values fit with Equation 4 ($n = 7$). Half-maximal availability (V_{50}) occurred at −70.8 ± 0.3 mV with a k of 6 mV. In the presence of L-cysteine, the V_{50} was −69 ± 0.1 mV with a k of 5.2 mV. In the paired-pulse protocol used to assess the voltage dependence of steady-state inactivation, T-type currents were recorded at −30 mV after 3.5-s-lasting prepulses to potentials ranging from −95 to −50 mV. Normalized data for both the voltage dependence of activation and steady-state inactivation were fit with single Boltzmann functions (Eqs. 3, 4). ***G***, L-Cysteine increased the window period for T-type currents in T-rich cells as shown by the increased area of overlap beneath the Boltzmann distributions describing voltage-dependent activation and steady-state inactivation (data have been normalized for conductance to clearly depict the shift in availability). ***H***, Simulation of neuronal excitability based on the biophysical properties of T-type currents in T-rich cells under control conditions or in the presence of L-cysteine. Computer modeling was performed using the NEURON program and a model of thalamocortical relay neurons as described by Destexhe et al. (1998), modified to incorporate the biophysical parameters of T-type currents in T-rich cells as described in ***A–G***. Firing was triggered by a 2 ms, 1.7 nA stimulus from a membrane potential of −65 mV.

within the size range (≤35 μm) that comprises the majority of the capsaicin-sensitive and ATP-sensitive nociceptor population (Caterina and Julius, 2001; Petruska et al., 2000, 2002).

A majority of T-rich cells showed a hyperpolarizing response to 5-HT. This has been described previously for capsaicin-sensitive Aδ- and C-fibers in experiments using sharp electrodes to record from intact DRG–sciatic nerve preparations (Todorovic and Anderson, 1992). Notably, the 5-HT-evoked hyperpolarization was sufficient to produce deinactivation of T-type channels in most T-rich cells. In CNS neurons, T-type channels are commonly deinactivated after membrane hyperpolarization induced by inhibitory postsynaptic potentials (Perez-Reyes, 2003). However, a similar mechanism for the deinactivation of T-type channels in DRG neurons has not been described previously. 5-HT is known to be locally present in the DRG, skin, and spinal cord (for review, see Sommer, 2004). Thus, it is possible that 5-HT may contribute to membrane hyperpolarization and subsequent deinactivation of T-type Ca^{2+} channels *in vivo*.

As mentioned above, nociceptors can be subdivided on the basis of their ability to bind IB_4; this suggests that subpopulations of nociceptors may have distinct functions (Snider and McMahon, 1998; Stucky and Lewin, 1999). Although subsets of both IB_4-negative and -positive cells are believed to respond to noxious chemical, thermal, and mechanical stimuli, recent studies suggest that these subpopulations may contribute differentially to nociception. In general, IB_4-negative cells project to the most superficial layers of the spinal cord dorsal horn (lamina I and outer lamina II) and appear to be the major effectors of inflammatory pain, releasing their stores of proinflammatory peptides after activation. In contrast, genetic studies suggest that IB_4-positive, nonpeptidergic nociceptors project primarily to inner lamina II of the dorsal horn and are integral to the development of chronic pain after nerve injury. Because a majority of T-rich cells are IB_4 positive, these cells may represent, at least in part, a cellular substrate for the described contribution of T-type Ca^{2+} channels to neuropathic pain in animal models (Dogrul et al., 2003; Flatters and Bennett, 2004; Todorovic et al., 2004a; Bourinet et al., 2005).

We have demonstrated previously that L-cysteine acts as a potent agonist of T-type channels *in vitro* and induces mechanical and thermal hyperalgesia when injected into peripheral receptive fields *in vivo* (Todorovic et al., 2001, 2004a). Here, we continued by demonstrating L-cysteine-evoked enhancement of excitability in T-rich cells. L-Cysteine greatly increased the size of ADPs in T-rich cells, sometimes resulting in a burst of APs crowning the augmented ADP. In addition, L-cysteine significantly lowered the threshold for excitability in T-rich cells, as evidenced by the reduced stimulus necessary to evoke an AP in the presence of L-cysteine. These results provide the first direct evidence that T-type channels contribute to the control of nociceptor excitability in at least one subpopulation of nociceptors and also suggest a possible mechanistic substrate for the hyperalgesic effects of L-cysteine *in vivo*. In addition, evidence suggests that increased somatic excitability in sensory neurons is important for the initiation and maintenance of central sensitization in

the spinal cord, which is a suggested physiological correlate for neuropathic pain (for review, see Levine et al., 1993) (Coderre et al., 1993; Caterina and Julius, 2001; Bhave and Gereau, 2004). Thus, information concerning the contribution of T-type channels to peripheral sensitization in the DRG could help to define the role of these channels in chronic pain and may aid in the development of novel pain therapies. The latter is particularly important given the fact that chronic pain affects ~1.5% of the adult population in the United States and is often unresponsive to currently available treatments (Bennett, 1998).

L-Cysteine augments T-type currents in T-rich cells at concentrations between 10 and 100 μM. Because free L-cysteine concentrations are reported to exist in this range in blood (Suliman et al., 1997), it appears that L-cysteine may be an important modulator of excitability in T-rich cells *in vivo*. Furthermore, it is possible that L-cysteine is locally present (Persson et al., 2002) or released from the blood vessels and/or skin cells at injury sites, resulting in upregulation of T-type current and, subsequently, sensitization of T-rich nociceptors *in vivo*.

It is well documented that T-type channels in CNS neurons can generate low-threshold Ca^{2+} spikes, which in turn promote neuronal burst firing (Llinas, 1988; Huguenard, 1996) (for review, see Perez-Reyes, 2003). Our present data indicate that a similar phenomenon may exist in T-rich cells. Furthermore, we demonstrate that L-cysteine shifts the voltage dependence of activation to more hyperpolarized potentials with very little effect on steady-state inactivation. By shifting activation parameters to more hyperpolarized potentials, L-cysteine widens the T-type window period, ultimately leading to a greater probability of channel opening. Thus, the effects of L-cysteine on the excitability of T-rich cells could in part result from a gating shift in the voltage dependence of T-type current activation.

The NEURON model was developed for studies of the roles of T-type currents in the excitability of thalamocortical neurons (Destexhe et al., 1998). Our biophysical data from T-type currents in T-rich cells show many similarities to the biophysical properties of T-type currents in CNS neurons (i.e., voltage- and time-dependent activation and inactivation and a substantial window period) (Coulter et al., 1989). Even small changes in the window period of thalamocortical T-type channels can have important functional effects on excitability (Crunelli et al., 2005). Our simulations provide proof-of-principle support for a similar occurrence in sensory neurons and suggest that the effects of L-cysteine on the voltage dependence of T-type channel availability alone may be sufficient to produce lower thresholds for excitability. Together, our findings strongly suggest that T-type Ca^{2+} channels are important in the control of excitability of a novel subpopulation of T-rich nociceptors and may contribute to pain symptoms such as allodynia and hyperalgesia *in vivo*.

References

Bennett GJ (1998) Neuropathic pain: new insights, new interventions. Hosp Pract (Off Ed) 33:101–110.

Bhave G, Gereau RW (2004) Posttranslational mechanisms of peripheral sensitization. J Neurobiol 61:88–106.

Bourinet E, Alloui A, Monteiol A, Barrere C, Couette B, Poirot O, Pages A, McRory J, Snutch TP, Eschalier A, Nargeot J (2005) Silencing of the $Ca_v3.2$ T-type calcium channel gene in sensory neurons demonstrates its major role in nociception. EMBO J 24:315–324.

Cardenas CG, Del Mar LP, Scroggs RS (1995) Variation in serotonergic inhibition of calcium channel currents in four types of rat sensory neurons differentiated by membrane properties. J Neurophysiol 74:1870–1879.

Cardenas CG, Mar LP, Vysokanov AV, Arnold PB, Cardenas LM, Surmeier DJ, Scroggs RS (1999) Serotonergic modulation of hyperpolarization-activated current in acutely isolated rat dorsal root ganglion neurons. J Physiol (Lond) 518:507–523.

Caterina MJ, Julius D (2001) The vanilloid receptor: a molecular gateway to the pain pathway. Annu Rev Neurosci 24:487–517.

Caterina MJ, Schumacher MA, Tominaga M, Rosen TA, Levine JD, Julius D (1997) The capsaicin receptor: a heat-activated ion channel in the pain pathway. Nature 389:816–824.

Catterall WA (2000) Structure and regulation of voltage-gated Ca^{2+} channels. Annu Rev Cell Dev Biol 16:521–555.

Coderre TJ, Katz J, Vaccarino AL, Melzack R (1993) Contribution of central neuroplasticity to pathological pain: review of clinical and experimental evidence. Pain 52:259–285.

Coulter DA, Huguenard JR, Prince DA (1989) Calcium currents in rat thalamocortical relay neurons: kinetic properties of the transient, low threshold current. J Physiol (Lond) 414:587–604.

Crunelli V, Tóth TI, Cope DW, Blethyn K, Hughes SW (2005) The "window" T-type calcium current in brain dynamics of different behavioural states. J Physiol (Lond) 562:121–129.

Destexhe A, Contreras D, Steriade M (1998) Mechanisms underlying the synchronizing action of corticothalamic feedback through inhibition of thalamic relay cells. J Neurophysiol 79:999–1016.

Dogrul A, Gardell LR, Ossipov MH, Tulunay FC, Lai J, Porecca F (2003) Reversal of experimental neuropathic pain by T-type calcium channel blockers. Pain 105:159–168.

Dubreuil A, Boukhaddaoui H, Desmadryl G, Martinez-Salgado C, Moshourab R, Lewin GR, Caroll P, Valmier J, Scamps F (2004) Role of T-type calcium current in identified D-hair mechanoreceptor neurons studied *in vitro*. J Neurosci 24:8480–8484.

Flatters SJL, Bennett GJ (2004) Ethosuximide reverses paclitaxel- and vincristine-induced painful peripheral neuropathy. Pain 109:150–161.

Hodgkin AL, Huxley AF (1952) A quantitative description of membrane current and its application to conduction and excitation in nerve. J Physiol (Lond) 117:500–544.

Huguenard JR (1996) Low threshold calcium currents in central nervous system neurons. Annu Rev Physiol 58:329–348.

Lee KH, Chung K, Chung JM, Coggeshall RE (1986) Correlation of cell body size, axon size, and signal conduction velocity for individually labelled dorsal root ganglion cells in the cat. J Comp Neurol 15:335–346.

Levine JD, Fields HL, Basbaum AI (1993) Peptides and the primary afferent nociceptors. J Neurosci 13:2273–2286.

Llinas RR (1988) The intrinsic electrophysiological properties of mammalian neurons: insights into central nervous system function. Science 242:1654–1664.

McCleskey EW, Gold MS (1999) Ion channels of nociception. Annu Rev Physiol 61:835–856.

Miller RJ (1998) Presynaptic receptors. Annu Rev Pharmacol Toxicol 38:201–227.

Perez-Reyes E (2003) Molecular physiology of low-voltage-activated T-type calcium channels. Physiol Rev 83:117–161.

Persson B, Andersson A, Hultberg B, Hansson C (2002) The redox state of glutathione, cysteine and homocysteine in the extracellular fluid in the skin. Free Radic Res 36:151–156.

Petruska JC, Napaporn J, Johnson RD, Gu JG, Cooper BY (2000) Subclassified acutely dissociated cells of rat DRG: histochemistry and patterns of capsaicin-, proton-, and ATP-activated currents. J Neurophysiol 84:2365–2379.

Petruska JC, Napaporn J, Johnson RD, Gu JG, Cooper BY (2002) Chemical responsiveness and histochemical phenotype of electrophysiologically classified cells of the adult rat dorsal root ganglion. Neuroscience 115:15–30.

Schroeder JE, Fischbach PS, McCleskey EW (1990) T-type calcium channels: heterogeneous expression in rat sensory neurons and selective modulation by phorbol esters. J Neurosci 10:947–951.

Scroggs RS, Fox AP (1992) Calcium current variation between acutely isolated adult rat dorsal root ganglion neurons of different size. J Physiol (Lond) 445:639–658.

Snider WD, McMahon SB (1998) Tackling pain at the source: new ideas about nociceptors. Neuron 20:629–632.

Sommer C (2004) Serotonin in pain and analgesia. Mol Neurobiol 30:117–125.

Stucky CL, Lewin GR (1999) Isolectin B4-positive and -negative nociceptors are functionally distinct. J Neurosci 19:6497–6505.

Suliman ME, Anderstam B, Lindholm B, Bergstrom J (1997) Total, free, and protein-bound sulfur amino acids in uremic patients. Nephrol Dial Transplant 12:2332–2338.

Todorovic S, Anderson SG (1992) Serotonin preferentially hyperpolarizes capsaicin-sensitive C type sensory neurons by activating 5-HT1A receptors. Brain Res 585:212–218.

Todorovic SM, Lingle CJ (1998) Pharmacological properties of T-type Ca^{2+} current in adult rat sensory neurons: effects of anticonvulsant and anesthetic agents. J Neurophysiol 79:240–252.

Todorovic SM, Prakriya M, Nakashima YM, Nilsson KR, Han M, Zorumski CF, Covey DF, Lingle CJ (1998) Enantioselective blockade of t-type Ca^{2+} current in adult rat sensory neurons by a steroid that lacks γ-aminoutyric acid-modulatory activity. Mol Pharmcol 54: 918–927.

Todorovic SM, Jevtovic-Todorovic V, Meyenburg A, Mennerick S, Perez-Reyes E, Romano C, Olney JW, Zorumski CF (2001) Redox modulation of T-type calcium channels in rat peripheral nociceptors. Neuron 31:75–85.

Todorovic SM, Meyenburg A, Jevtovic-Todorovic V (2004a) Redox modulation of peripheral T-type Ca^{2+} channels in vivo: alteration of nerve injury-induced thermal hyperalgesia. Pain 109:328–339.

Todorovic SM, Pathirathna S, Brimelow BC, Jagodic MM, Ko SH, Jiang X, Nilsson KR, Zorumski CF, Covey DF, Jevtovic-Todorovic V (2004b) 5beta-reduced neuroactive steroids are novel voltage-dependent blockers of T-type Ca^{2+} channels in rat sensory neurons in vitro and potent peripheral analgesics in vivo. Mol Pharmacol 66:1223–1235.

White G, Lovinger DM, Weight FF (1989) Transient low-threshold Ca^{2+} current triggers burst firing through an afterdepolarizing potential in an adult mammalian neuron. Proc Natl Acad Sci USA 86:6802–6806.

Wilson DL, Morimoto K, Tsuda Y, Brown AM (1983) Interaction between calcium ions and surface charge as it relates to calcium currents. J Membr Biol 72:117–130.